

British Journal of Ophthalmology

Extra-ocular muscle positions in anterior plagiocephaly; V-pattern strabismus explained using geometric morphometrics

Journal:	<i>British Journal of Ophthalmology</i>
Manuscript ID	bjophthalmol-2019-314989.R1
Article Type:	Clinical science
Date Submitted by the Author:	n/a
Complete List of Authors:	Touzé, Romain; Hopital Necker-Enfants Malades, Ophthalmology Heuzé, Yann; CRNS, Université de Bordeaux Robert, Matthieu; Hopital universitaire Necker-Enfants malades Maladies rares et chroniques, Ophthalmology Bremond Gignac, Dominique; University Hospital, Necker enfants maladies, Ophthalmology; Paris V René Descartes University, CNRS Unit FR3636 Roux, Charles-Joris; Hopital Necker-Enfants Malades, Pediatric Radiology James, Cyril; Hopital Necker-Enfants Malades, Neurosurgery; Clinique Marcel Sembat, Neurosurgery Paternoster, Giovanna; Hopital Necker-Enfants Malades, Neurosurgery Arnaud, Eric; Hopital Necker-Enfants Malades, Neurosurgery; Clinique Marcel Sembat, Neurosurgery Khonsari, Roman Hossein; Hopital Necker-Enfants Malades, Maxillo-facial and plastic surgery unit
Keywords:	Child health (paediatrics), Imaging, Muscles, Orbit, Treatment Surgery

SCHOLARONE™
Manuscripts

1		
2		
3	1	Title page
4		
5	2	Extra-ocular muscle positions in anterior plagiocephaly; V-pattern strabismus
6	3	explained using geometric morphometrics
7		
8		
9	4	Short title V-pattern strabismus in anterior plagiocephaly
10		
11	5	
12		
13	6	Romain Touzé ^{1*} , Yann Heuzé ² , Matthieu P. Robert ^{1,3} , Dominique Brémond-Gignac ¹ , Charles-Joris
14	7	Roux ⁴ , Cyril James ^{5,6} , Giovanna Paternoster ⁵ , Eric Arnaud ^{5,6} , Roman Hossein Khonsari ⁷
15		
16	8	1. Service d’ophtalmologie, Hôpital Universitaire Necker – Enfants Malades, Assistance
17	9	Publique – Hôpitaux de Paris ; Université de Paris, Sorbonne Paris Cité ; Paris, France
18		
19	10	2. CNRS, Université de Bordeaux, MCC, PACEA, UMR5199, Pessac, France
20		
21	11	3. COGNAC-G, UMR 8257 CNRS-SSA-Université de Paris, Paris, France
22	12	4. Service de radiologie, Hôpital Universitaire Necker – Enfants Malades, Assistance
23	13	Publique – Hôpitaux de Paris ; Université de Paris, Sorbonne Paris Cité ; Paris, France
24		
25	14	5. Service de neurochirurgie, Unité Fonctionnelle de Chirurgie Craniofaciale, Hôpital
26	15	Universitaire Necker – Enfants Malades, Assistance Publique – Hôpitaux de Paris ; Centre de
27	16	Référence des Malformations Craniofaciale CRANIOST, Filière Maladies Rares TeteCou ;
28	17	Université de Paris, Sorbonne Paris Cité ; Paris, France
29		
30	18	6. Clinique Marcel Sembat, Ramsay – Générale de Santé, Boulogne-Billancourt, France
31	19	7. Service de chirurgie maxillo-faciale et chirurgie plastique, Hôpital Universitaire Necker
32		– Enfants Malades, Assistance Publique – Hôpitaux de Paris ; Centre de Référence des
33	20	Malformations Rares de la Face et de la Cavité Buccale MAFACE, Filière Maladies Rares
34	21	TeteCou ; Université de Paris, Sorbonne Paris Cité ; Paris, France
35	22	
36	23	
37		
38		
39	24	
40	25	
41		
42	26	Keywords: Child health (paediatrics); Imaging; Muscles; Orbit; Treatment Surgery
43	27	
44	28	Number of Tables: 1
45	29	Number of Figures: 4
46		
47	30	Word count of Abstract: 243
48	31	Word count of Paper: 2440
49	32	
50	33	
51		
52	34	
53	35	
54		
55	36	
56	37	
57		
58	38	
59	39	
60	40	

Corresponding Author:

Dr Romain Touzé

Service d'ophtalmologie, Hôpital Universitaire Necker - Enfants Malades, 149, Rue de
Sèvres, 75015 Paris. FranceEmail r.touze.rt@gmail.com

Tel + 33629654980

1
2
3
4
5
6
7
8
9
10
11
12
13
14
15
16
17
18
19
20
21
22
23
24
25
26
27
28
29
30
31
32
33
34
35
36
37
38
39
40
41
42
43
44
45
46
47
48
49
50
51
52
53
54
55
56
57
58
59
60

Synopsis:

This study reports statistically abnormal extra-oculomotor muscles positions within the orbit of patients with anterior plagiocephaly using the geometric morphometrics, in order to better understand strabismus in this pathology especially V-pattern.

79 Abstract

80 Introduction

81 Ophthalmological involvement in anterior plagiocephaly (AP) due to unicoronal synostosis
82 (UCS) raises management challenges. Two abnormalities of the extra-ocular muscles (EOM)
83 are commonly reported in UCS without objective quantification: (1) malposition of the trochlea
84 of the superior oblique muscle and (2) excyclorotation of the eye. Here we aimed to assess the
85 positions of the EOM in AP, using geometric morphometrics based on magnetic resonance
86 imaging (MRI) data.

87 Materials and Methods

88 Patient files were listed using Dr WareHouse, a dedicated big data search engine. We included
89 all patients with AP managed between 2013 and 2018, with an available digital pre-operative
90 MRI. MRIs from age-matched controls without craniofacial conditions were also included. We
91 defined 13 orbital and skull base landmarks in order to model the 3D position of the EOM.
92 Cephalometric analyses and geometric morphometrics with Procrustes superimposition and
93 principal component analysis were used with the aim of defining specific EOM anomalies in
94 UCS.

95 Results

96 We included 15 pre-operative and 7 post-operative MRIs from patients with UCS and 24 MRIs
97 from age-matched controls. Cephalometric analyses, Procrustes superimposition and distance
98 computations showed a significant shape difference for the position of the trochlea of the
99 superior oblique muscle and an excyclorotation of the EOM.

100 Conclusion

101 Our results confirm that UCS-associated anomalies of the superior oblique muscle function are
102 associated with a malposition of its trochlea in the roof of the orbit. This clinical anomaly
103 supports the importance of MRI imaging in the surgical management of strabismus in patients
104 with UCS.

105

1
2
3
4
5
6
7
8
9
10
11
12
13
14
15
16
17
18
19
20
21
22
23
24
25
26
27
28
29
30
31
32
33
34
35
36
37
38
39
40
41
42
43
44
45
46
47
48
49
50
51
52
53
54
55
56
57
58
59
60

Introduction

Craniosynostoses are often associated with strabismus. The management of these specific types of strabismus is a clinical challenge, especially in anterior plagiocephaly (AP) caused by unicoronal synostosis (UCS). UCS is the third most common single-suture craniosynostosis and is associated with the premature unilateral fusion of a coronal suture. Craniofacial anomalies in UCS include a larger orbit on the affected side, a shift of the petrous bone towards the fused suture, compensatory growth of the contralateral forehead and temporal bone, and contralateral deviation of the vomer and nasal pyramid.[1]

Ocular involvement is frequent in UCS and includes extra-ocular muscle (EOM) dysfunction with cyclovertical strabismus, astigmatism - usually contralateral to the UCS, due to the compensatory deformations of the contralateral bones - with anisometropia, and amblyopia. The prevalence of ocular abnormalities ranges from 50 to 65% in this condition.[2–4] This high prevalence underlines the need for a systematic ophthalmological clinical screening for patients with UCS within multidisciplinary craniofacial teams, in order to prevent, detect, and treat the amblyopia.

The most common type of strabismus in UCS is referred to as the V-pattern, which is defined by a vertical incomitance with a distance between both eyes larger in upgaze than in downgaze.[2,5] Two hypotheses have been proposed in the literature in order to explain the occurrence of V-pattern oculomotor anomalies in UCS: (1) excyclorotation of the rectus muscle and (2) inferior oblique overaction associated with superior oblique underaction.[1,2,6,7]

Here we assessed the positions of the EOM in patients with UCS and controls, based on MRI data and geometric morphometric analyses, and screened for clinically relevant specificities of the muscular anatomy of UCS orbits.

1
2
3 129 Geometric morphometrics allowed us to acquire, process and analyze landmarks by preserving
4
5 130 their 3D inter-relationship. This approach was required as we had to compare non-trivial
6
7 131 shapes.[8] The framework used to assess our data was Procrustes superimposition followed by
8
9 132 Principal Component Analysis (PCA). Procrustes superimposition allowed comparing different
10
11 133 shapes by freely adjusting the position, orientation and scale parameters using translations,
12
13 134 reflections and rotations.[9] PCA was used to reduce the large number of variables responsible
14
15 135 for shape differences into a small number of principal variables with geometric
16
17 136 correspondence.[10]
18
19
20
21
22 137 Our aim was to find anatomical bases for the V-pattern strabismus. More precisely, we assessed
23
24 138 the 3D modifications in the positions of EOM in UCS and the effects of fronto-orbital
25
26 139 advancement surgery on these positions.
27
28
29

30 140
31
32
33
34
35
36
37
38
39
40
41
42
43
44
45
46
47
48
49
50
51
52
53
54
55
56
57
58
59
60

1
2
3 141 **Material and Methods**
4

5
6 142
7

8
9 143 *Clinical data*
10

11
12 144 We retrospectively included patients with isolated UCS and with at least one available digital
13
14 145 pre-operative craniofacial magnetic resonance imaging (MRI), managed in our tertiary center
15
16 146 (French National Reference Center for Craniofacial Malformations - CRANIOST) between
17
18 147 2013 and 2018, using Dr Warehouse search engine.[11] We excluded patients with complex
19
20 148 and syndromic craniosynostosis and deformational plagiocephaly. Age-matched control
21
22 149 patients without craniofacial anomalies were also retrospectively included. We analyzed the
23
24 150 effects of fronto-orbital advancement surgery based on post-operative MRIs for included
25
26 151 patients, when available. For image analysis purposes, we mirrored patients with left UCS in
27
28 152 order to consider a cohort of patients with right UCS only.[12] All patients with UCS benefited
29
30 153 from fronto-orbital advancement.
31
32
33
34

35
36 154
37

38
39 155 *Morphometrics*
40

41
42 156 Landmarking was performed using Avizo 6.4.0 (Thermo Fisher Scientific, Waltham,
43
44 157 Massachusetts, USA). Landmarks were placed using Multi Planar Reconstruction (MPR) on
45
46 158 Cube T1-weighted or Cube T2-weighted sequences. Twelve bilateral orbital landmarks were
47
48 159 defined: (1; 5) right and left lateral rectus; (2; 6) right and left superior rectus; (3; 7) right and
49
50 160 left medial rectus; (4; 8) right and left inferior rectus; (9; 10) right and left optic nerve; (11; 12)
51
52 161 right and left superior oblique trochlea. One extra-orbital landmark was also defined: (13)
53
54 162 chiasma (Table 1). Landmarks 1-10 were placed using coronal views, on the plane immediately
55
56
57
58
59
60

behind the two globes (Figure 1). Pulleys of recti muscles were described in dynamic MRI (IMROD) as encircling sleeves and rings of collagen in the tenon fascia.[13]

Table 1.

Number	Anatomical definition
1	Right lateral rectus chiasma
2	Right superior rectus
3	Right medial rectus
4	Right inferior rectus
5	Left lateral rectus chiasma
6	Left superior rectus
7	Left medial rectus
8	Left inferior rectus
9	Right optic nerve
10	Left optic nerve
11	Right superior oblique trochlea
12	Left superior oblique trochlea
13	Chiasma

Table 1. Orbital and extra-orbital landmarks used to model the 3D position of extra-ocular muscles in anterior plagiocephaly.

These pulleys represented the functional vector of EOMs and were located more proximal relative to muscle insertions. That's why we determined the coronal plane sectioning these pulleys to place landmarks concerning recti muscles. Landmarks 11 and 12 were defined using MPR after having localized the trochlea of the superior oblique muscle. Landmark 13 (chiasma) was placed using coronal sections.

We exported all landmark coordinates from Avizo to MorphoJ [14] in order to perform geometric morphometric analyses.[8] We extracted the shape information defined by the

1
2
3
4
5
6
7
8
9
10
11
12
13
14
15
16
17
18
19
20
21
22
23
24
25
26
27
28
29
30
31
32
33
34
35
36
37
38
39
40
41
42
43
44
45
46
47
48
49
50
51
52
53
54
55
56
57
58
59
60

landmarks and performed a generalized Procrustes superimposition.[9] Procrustes shape coordinates were analyzed using a principal components analysis (PCA).[10] Shape differences between groups were assessed based on Procrustes distances (d) with a permutation test of 10,000 rounds to test the statistical significance of d . [8]

We furthermore performed cephalometrics analyses in 2D defining angles and linear distances between landmarks in using coronal and axial planes. These angles and distances were determined using Euclidian distances and scalar products, and compared between UCS and controls. We defined two vectors named u (landmark 2 to 4) and v (landmark 1 to 3) in the coronal plane. Angle α between u and v was computed using the scalar product. We furthermore computed the angles β between u and the x-axis, and the angle γ between v and the x-axis (Resumed in the Figure 3).

Data analysis

Data analysis was performed using R3.3.3.[15] Comparisons of means were performed using a Wilcoxon test, depending on the data distribution and significance was defined for $p < 0.05$. We performed a reproducibility assessment based on a subset of 10 normal MRIs. Two operators (for the interobserver reproducibility) (RT and RHK) landmarked these MRIs three consecutive times (intraobserver reproducibility). The *concordance correlation coefficient* (CCC) agreement of Lin [16] was computed for each operator and landmark. An *overall concordance correlation coefficient* (OCCC) was also computed.[17] CCC and OCCC values above 0.99 corresponded to excellent reproducibility of landmark placement.[16]

196

197 Results

198 We selected 26 patients with UCS; we excluded 10 patients because of low quality MRI images
199 and 1 patient with a late diagnosis of complex craniosynostosis to finally include 15 patients
200 with MRI data before any cranio-facial surgery. The mean age of the 15 remaining patients (30
201 orbits) was 11.9 ± 5.7 months (4-22 months). We included 24 (48 orbits) age-matched controls,
202 with a mean age of 13.4 ± 5.8 months (6-23 months) ($p=0.61$). Among the 15 included patients
203 with UCS, 7 had a digital post-operative MRI (14 orbits) performed 1 month after the surgical
204 procedure (fronto-orbital advancement). The mean age of patients with post-operative MRIs
205 was 17 ± 5.3 months (13-25 months). None of these 7 patients had EOM surgery performed
206 before post-operative MRIs.

207 The CCC for each landmark and OCCC were above 0.99, indicating reliable landmark
208 placement for all landmarks and the two operators.

209 The PCA found shape's difference between both groups. The first five principal components
210 (PCs) accounted for more than 70% of the total variance (Supplementary Figure 1). Both groups
211 were well separated with the two first PCs (Supplementary Figure 2). The Procrustes distance
212 between UCS and control was significant ($d=0.11$, $p < 0.01$). We observed an abnormal location
213 of the superior oblique trochlea in the UCS orbit, corresponding to a lateral, superior and
214 posterior displacement within the orbit (Figure 2-3). We furthermore observed a significant
215 excyclorotation in the UCS group, affecting the recti muscles, more pronounced on the side
216 where the suture was closed. In UCS, the superior rectus was displaced laterally, the inferior
217 rectus was displaced medially, the lateral rectus downward, and the medial rectus upward in
218 the coronal plane (Figure 3).

1
2
3 219 Euclidian distances between landmark 11 (right superior oblique trochlea) and landmark 9
4
5 220 (right optic nerve) were smaller in the UCS group compared to control group: respectively 18.9
6
7 221 mm \pm 1.7 mm vs. 20.6 mm \pm 1.4 mm ($p = 0.002$; IC95% [0.77; ∞]), which confirmed the lateral
8
9 222 (coronal plane) and posterior (axial plane) displacement of the trochlea within the orbit.
10
11
12
13 223 Mean α was significantly different between control and UCS groups: $81.3^\circ \pm 4.6^\circ$ vs 74.3°
14
15 224 $\pm 8.6^\circ$ respectively ($p=0.008$; IC95% [2.1; 12.2]). Mean β was significantly different between
16
17 225 control and UCS groups: $82.4^\circ \pm 5.2^\circ$ vs $66.3^\circ \pm 8.1^\circ$ respectively ($p<0.001$; IC95% [11.1;
18
19 226 20.9]). Mean γ was significantly different between control and UCS groups: $0.9^\circ \pm 3.7^\circ$ vs 7.9°
20
21 227 $\pm 7.2^\circ$ respectively ($p<0.001$; IC95% [-13.0; -4.7]). α and β were smaller in the UCS group
22
23 228 relative to controls; γ values were larger in the UCS group relative to controls.
24
25
26
27 229 Among the 15 patients included, 7 patients had an MRI performed before and after Fronto-
28
29 230 facial advancement. In this subgroup of patients, we observed a qualitative decrease of the
30
31 231 excyclorotation of the recti muscles after surgery: the superior oblique muscle was displaced
32
33 232 downward and medially compared to the pattern before surgery, which corresponded to a trend
34
35 233 towards normalization (Figure 4). Nevertheless, we could not confirm this shape modification
36
37 234 quantitatively because we found a Procrustes distance at 0.05 with a p-value (10000
38
39 235 permutations) of 0.07.
40
41
42
43
44
45
46
47
48
49
50
51
52
53
54
55
56
57
58
59
60

236 Discussion

237 The management of strabismus in craniosynostosis, and particularly in UCS, is a challenge as
238 its mechanisms are not clearly established and because of the massive orbital remodeling caused
239 by craniofacial surgical procedures, such as fronto-orbital advancement.

240 The high prevalence of strabismus in UCS is well-established: in their cohort of 59 UCS
241 patients, MacIntosh *et al.* [2] found 57.6% of strabismus, 61% of which were esotropia with a
242 vertical component, with 50.8% of inferior oblique overaction / superior oblique underaction.

243 In a recent review Ron et Dagi [18] summarized all hypotheses explaining V-pattern strabismus
244 in craniosynostoses and pinpointed two main theories as the most satisfactory : (1) inferior
245 oblique overaction / superior oblique underaction induced by the orbital deformation, and (2)
246 excyclorotation of the recti EOM, also induced by the orbital deformation. Nischal *et al.* [19]
247 proposed a three-step theory in order to explain the origins of this specific type of strabismus
248 in UCS: (1) frontal retrusion on the side with coronal synostosis, (2) secondary displacement
249 of the trochlea of the superior oblique muscle, (3) causing a mechanical disadvantage for the
250 superior oblique muscle and an overaction of the inferior oblique. However, Cheng *et al.* [20]
251 argued that the V-pattern vertical component or the upshoot in adduction could not be explained
252 by the inferior oblique overaction / superior oblique underaction only. For these authors, the
253 excyclorotation induced by the deformation of the orbit was also involved in the origin of the
254 strabismus. They demonstrated the excyclorotation of the EOM in several cases of
255 craniosynostosis - the medial rectus being displaced upward, the lateral rectus downward, the
256 inferior rectus medially and the superior rectus laterally. Tan *et al.* [21] studied the upshoot in
257 adduction in order to determine its causes, based on a cohort of 40 patients with various forms
258 of craniosynostosis, including 9 patients with UCS. Among these 9 patients with UCS, 6
259 patients had an upshoot in adduction. They found that the angle of excyclorotation was more

1
2
3 260 pronounced in patients with upshoot in adduction, based on comparisons with the non-affected
4
5 261 side.
6
7
8 262 Here, we provide for the first-time quantitative data on the average position of the EOM in the
9
10 263 UCS orbit. We found a significant upward, lateral and backward displacement of the trochlea
11
12
13 264 of the oblique superior muscle. According to the vectorial action of the oblique superior muscle,
14
15 265 these displacements were most probably associated with a weaker action of the oblique superior
16
17 266 muscle, because the pulley effect of the trochlea was less efficient and a more posterior trochlea
18
19
20 267 induced an upward drift of the globe. We also demonstrated an excyclorotation, in particular
21
22 268 affecting the superior rectus (laterally displaced) and the inferior rectus (medially displaced).
23
24 269 To our knowledge, this is the first evidence of EOM displacements in UCS based on 3D MRI
25
26
27 270 data, and the first quantitative and objective support of the current theories on the origins of
28
29 271 strabismus in UCS.
30
31
32 272 The displacement of the superior oblique trochlea can induce a pseudo-superior oblique palsy.
33
34 273 As any superior oblique palsy - or pseudo superior oblique palsy - causes a true excyclorotation
35
36 274 of the globe, [22] hence of the EOM, it is difficult to assess whether the excyclorotation of the
37
38 275 EOM found in these patients is an effect of the pseudo-superior oblique palsy resulting from a
39
40 276 trochlea displacement, or a direct effect of a bony orbit rotation. In order to answer this question,
41
42 277 further study could aim at correlating the bony orbit rotation and the EOM excyclorotation in
43
44 278 UCS.
45
46
47
48
49 279 Orbital imaging using MRI in craniosynostosis is a valuable tool for the assessment of
50
51 280 strabismus.[23–25] The absence of rectus and/or oblique muscles has been reported in
52
53 281 craniosynostosis cases and should be diagnosed before the surgery.[26] Further studies are also
54
55 282 needed to better describe the EOM phenotype in other forms of non-syndromic and syndromic
56
57 283 craniosynostosis.
58
59
60

According to the literature, surgery on oculomotor muscles should be performed after craniofacial procedures, such as fronto-orbital advancement.[1,19,25,27,28] In a recent review, Alfort *et al.* [29] underlined the specific risk of strabismus secondary to fronto-orbital advancement. Patients are under 12 months of age when undergoing this procedure and oculomotor muscle surgery is usually performed later in age. Our data showed a trend towards normalization for excyclorotation and trochlea position after fronto-orbital advancement in a subgroup of 7 patients. Nevertheless, we were not able to demonstrate this morphological modification and correlate it with clinical effects on strabismus, due to an insufficient number of patients and to the impossibility to precisely quantify cyclovertical strabismus characteristics below one year of age.

To date, no guidelines exist for the management of strabismus in craniosynostoses. The usual procedure to treat inferior oblique overaction consists in weakening the inferior oblique muscle. Some authors, such as Tan *et al.* [21], have suggested that in cases with significant excyclorotation, a transposition of the inferiorly displaced lateral rectus muscle could be more appropriate to correct the V-pattern.

Limitations

One of the main potential limitations of this study relates to the accuracy of landmark placement. In order to evaluate this issue, we assessed intra- and inter-individual reproducibility of landmark placement, as described in the Material and Methods section, and showed the reliability of our landmark placement protocol.

In brief, we quantitatively demonstrated two main EOM modifications associated with UCS: (1) lateral, superior and posterior displacement of the superior oblique trochlea and (2) excyclorotation of the rectus muscles. These anatomical anomalies are reasonable candidates to explain the origins and specificities of strabismus in UCS.

1
2
3
4
5
6
7
8
9
10
11
12
13
14
15
16
17
18
19
20
21
22
23
24
25
26
27
28
29
30
31
32
33
34
35
36
37
38
39
40
41
42
43
44
45
46
47
48
49
50
51
52
53
54
55
56
57
58
59
60

Conclusion

We report the first detailed assessment of EOM positions in anterior plagiocephaly due to unicoronal synostosis. Strabismus in unicoronal synostosis has repeatedly been explained by weakness of the superior oblique muscle due to a malposition of its trochlea and excyclorotation of rectus muscles. Our study provides a quantitative proof of these two anomalies and supports the usual hypothesis formulated in the literature. It underlines the relevance of orbital imaging in the management of strabismus in patients with UCS.

316 **Funding Statement**

317 This research received no specific grant from any funding agency in the public, commercial or
318 not-for-profit sectors.

320 **Competing Interests**

321 None authors have a competing interest

323 **Contributorship Statement**

324 All authors made substantial contributions to conception and design, analysis and interpretation
325 of data; drafted or critically revised the article; and gave final approval of the version to be
326 published.

328 **Data Sharing**

329 N/A

331 **Acknowledgments**

332 Special thanks to strabologists Drs Mitra Goberville and Marie-Andrée Espinasse-Berrod.

333 **Ethical statement**

334 Patients were informed of the use of their medical data for this study.

335

References

1 Di Rocco C, Paternoster G, Caldarelli M, *et al.* Anterior plagiocephaly: epidemiology, clinical findings, diagnosis, and classification. A review. *Childs Nerv Syst* 2012;**28**:1413–22. doi:10.1007/s00381-012-1845-2

2 MacIntosh C, Wall S, Leach C. Strabismus in unicoronal synostosis: ipsilateral or contralateral? *J Craniofac Surg* 2007;**18**:465–469.

3 Eveleens JRJ, Mathijssen IM, Lequin MH, *et al.* Vertical Position of the Orbits in Nonsyndromic Plagiocephaly in Childhood and Its Relation to Vertical Strabismus: *J Craniofac Surg* 2011;**22**:135–8. doi:10.1097/SCS.0b013e3181f6f814

4 Gupta PC, Foster J, Crowe S, *et al.* Ophthalmologic findings in patients with nonsyndromic plagiocephaly. *J Craniofac Surg* 2003;**14**:529–532.

5 Samra F, Paliga JT, Tahiri Y, *et al.* The prevalence of strabismus in unilateral coronal synostosis. *Childs Nerv Syst* 2015;**31**:589–96. doi:10.1007/s00381-014-2580-7

6 Dagi LR, MacKinnon S, Zurakowski D, *et al.* Rectus muscle excyclorotation and V-pattern strabismus: a quantitative appraisal of clinical relevance in syndromic craniosynostosis. *Br J Ophthalmol* 2017;**101**:1560–5. doi:10.1136/bjophthalmol-2016-309996

7 Bagolini B, Campos EC, Chiesi C. Plagiocephaly Causing Superior Oblique Deficiency and Ocular Torticollis: A New Clinical Entity. *Arch Ophthalmol* 1982;**100**:1093–6. doi:10.1001/archopht.1982.01030040071012

8 Mitteroecker P, Gunz P. Advances in Geometric Morphometrics. *Evol Biol* 2009;**36**:235–47. doi:10.1007/s11692-009-9055-x

9 Rohlf FJ, Slice D. Extensions of the Procrustes Method for the Optimal Superimposition of Landmarks. *Syst Biol* 1990;**39**:40–59. doi:10.2307/2992207

10 Jolliffe I. Principal Component Analysis. In: Lovric M, ed. *International Encyclopedia of Statistical Science*. Berlin, Heidelberg: : Springer Berlin Heidelberg 2011. 1094–6. doi:10.1007/978-3-642-04898-2_455

11 Garcelon N, Neuraz A, Benoit V, *et al.* Improving a full-text search engine: the importance of negation detection and family history context to identify cases in a biomedical data warehouse. *J Am Med Inform Assoc* 2017;**24**:607–13. doi:10.1093/jamia/ocw144

12 Heuzé Y, Martínez-Abadías N, Stella JM, *et al.* Unilateral and bilateral expression of a quantitative trait: asymmetry and symmetry in coronal craniosynostosis. *J Exp Zool B Mol Dev Evol* 2012;**318**:109–122.

13 Kono R, Clark RA, Demer JL. Active pulleys: magnetic resonance imaging of rectus muscle paths in tertiary gazes. *Invest Ophthalmol Vis Sci* 2002;**43**:2179–2188.

- 14 Klingenberg CP. MorphoJ: an integrated software package for geometric morphometrics. *Mol Ecol Resour* 2011;**11**:353–7. doi:10.1111/j.1755-0998.2010.02924.x
- 15 Team RC. R: A language and environment for statistical computing. R Foundation for Statistical Computing, Vienna, Austria. 2012. URL *Httpwww R-Proj Org* 2018.
- 16 Lin LI-K. A Concordance Correlation Coefficient to Evaluate Reproducibility. *Biometrics* 1989;**45**:255–68. doi:10.2307/2532051
- 17 Barnhart HX, Haber M, Song J. Overall Concordance Correlation Coefficient for Evaluating Agreement Among Multiple Observers. *Biometrics* 2002;**58**:1020–7. doi:10.1111/j.0006-341X.2002.01020.x
- 18 Ron Y, Dagi LR. The etiology of V pattern strabismus in patients with craniosynostosis. *Int Ophthalmol Clin* 2008;**48**:215–223.
- 19 Nischal KK. Ocular aspects of craniofacial disorders. *Am Orthopt J* 2002;**52**:58–68.
- 20 Cheng H, Burdon MA, Shun-Shin GA, *et al*. Dissociated eye movements in craniosynostosis: a hypothesis revived. *Br J Ophthalmol* 1993;**77**:563–8. doi:10.1136/bjo.77.9.563
- 21 Tan KP, Sargent MA, Poskitt KJ, *et al*. Ocular Overelevation in Adduction in Craniosynostosis: Is It the Result of Excyclorotation of the Extraocular Muscles? *J Am Assoc Pediatr Ophthalmol Strabismus* 2005;**9**:550–7. doi:10.1016/j.jaapos.2005.07.004
- 22 Noorden GK von, Murray E, Wong SY. Superior Oblique Paralysis: A Review of 270 Cases. *Arch Ophthalmol* 1986;**104**:1771–6. doi:10.1001/archoph.1986.01050240045037
- 23 Clark RA. Orbital Imaging in Strabismus. *J Binocul Vis Ocul Motil* 2018;**68**:87–98. doi:10.1080/2576117X.2018.1486678
- 24 Clark RA, Demer JL. Magnetic Resonance Imaging of the Effects of Horizontal Rectus Extraocular Muscle Surgery on Pulley and Globe Positions and Stability. *Investig Ophthalmology Vis Sci* 2006;**47**:188. doi:10.1167/iovs.05-0498
- 25 Morax S. Oculo-motor disorders in craniofacial malformations. *J Maxillofac Surg* 1984;**12**:1–10. doi:10.1016/S0301-0503(84)80201-5
- 26 Diamond GR, Katowitz JA, Whitaker LA, *et al*. Variations in extraocular muscle number and structure in craniofacial dysostosis. *Am J Ophthalmol* 1980;**90**:416–418.
- 27 Yang B, Ni J, Li B. 3D morphological change of skull base and fronto-temporal soft-tissue in the patients with unicoronal craniosynostosis after fronto-orbital advancement. *Childs Nerv Syst* 2018;**34**:947–55. doi:10.1007/s00381-018-3721-1
- 28 Simon A, Bocquet E, Pellerin P, *et al*. Three-dimensional study of 31 cases of synostotic anterior plagiocephaly before and after surgical management the Lille protocol. *J Cranio-Maxillofac Surg* 2018;**46**:958–66. doi:10.1016/j.jcms.2018.03.014
- 29 Alford J, Derderian CA, Smartt JM. Surgical Treatment of Nonsyndromic Unicoronal Craniosynostosis. *J Craniofac Surg* 2018;**1**. doi:10.1097/SCS.00000000000004509

1
2
3 410
4
5
6 411
7
8 412
9
10
11
12
13
14
15
16
17
18
19
20
21
22
23
24
25
26
27
28
29
30
31
32
33
34
35
36
37
38
39
40
41
42
43
44
45
46
47
48
49
50
51
52
53
54
55
56
57
58
59
60

Figure legends

Figure 1. 3D positioning of the landmarks based on MRI images. A. Red line: section plane used to place rectus muscle landmarks. B. Rectus muscle landmarks (red dots) and optic nerve landmarks (dark green dots). C. Trochlea of superior oblique muscles (yellow circles). D,E. Trochlea of superior oblique muscles (yellow dots). F. Chiasma landmark (blue dot); rectus muscle landmarks (red dots); optic nerve landmarks (dark green dots); trochlea of superior oblique muscles (yellow dots).

Figure 2. A. Procrustes superimposition in axial view for controls; right trochlea of the superior oblique muscle: red arrow. B. Procrustes superimposition in coronal view for controls; right trochlea of the superior oblique muscle: red arrow. C. Procrustes superimposition in sagittal view for controls. D. Procrustes superimposition in axial view for anterior plagiocephaly; right trochlea of the superior oblique muscle: red arrow. E. Procrustes superimposition in coronal view for anterior plagiocephaly; right trochlea of the superior oblique muscle: red arrow. F. Procrustes superimposition in sagittal view for anterior plagiocephaly.

Figure 3. A. Landmarks in a control case displayed on a coronal MRI section. B. Landmarks in an anterior plagiocephaly case displayed on a coronal MRI section. Exocyclorotation quantified using angles α , β and γ ; right trochlea of superior oblique muscle: red arrow.

Figure 4. A. Coronal MRI section in anterior plagiocephaly before fronto-orbital advancement. B. Coronal MRI section in anterior plagiocephaly after fronto-orbital advancement. Qualitative correction of the position of the right trochlea of the superior oblique muscle (red arrow) and qualitative reduction of the exocyclorotation of rectus muscles.

1
2
3
4
5
6
7
8
9
10
11
12
13
14
15
16
17
18
19
20
21
22
23
24
25
26
27
28
29
30
31
32
33
34
35
36
37
38
39
40
41
42
43
44
45
46
47
48
49
50
51
52
53
54
55
56
57
58
59
60

Figure legends supplementary files

Figure 1. Variance

A diagram showing the percentages of total variance for which the principal components (PCs) account. The five first PCs represent more than 70% of the total difference between both groups.

Figure 2. PCA

Principal component analysis with Procrustes superimposition of the two groups (UCS) and control. We can observe difference with confidence ellipses concerning PC1 vs PC2; PC1 vs PC4; and PC1 vs PC5.

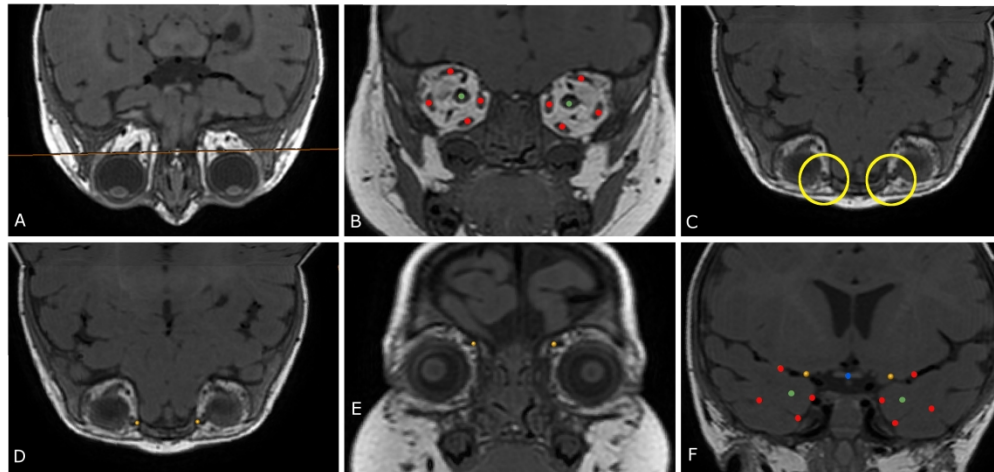


Figure 1. 3D positioning of the landmarks based on MRI images. A. Red line: section plane used to place rectus muscle landmarks. B. Rectus muscle landmarks (red dots) and optic nerve landmarks (dark green dots). C. Trochlea of superior oblique muscles (yellow circles). D,E. Trochlea of superior oblique muscles (yellow dots). F. Chiasma landmark (blue dot); rectus muscle landmarks (red dots); optic nerve landmarks (dark green dots); trochlea of superior oblique muscles (yellow dots).

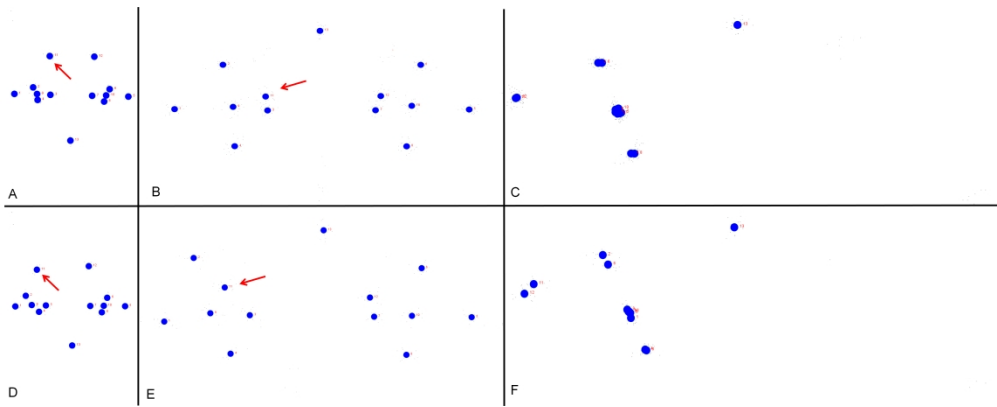
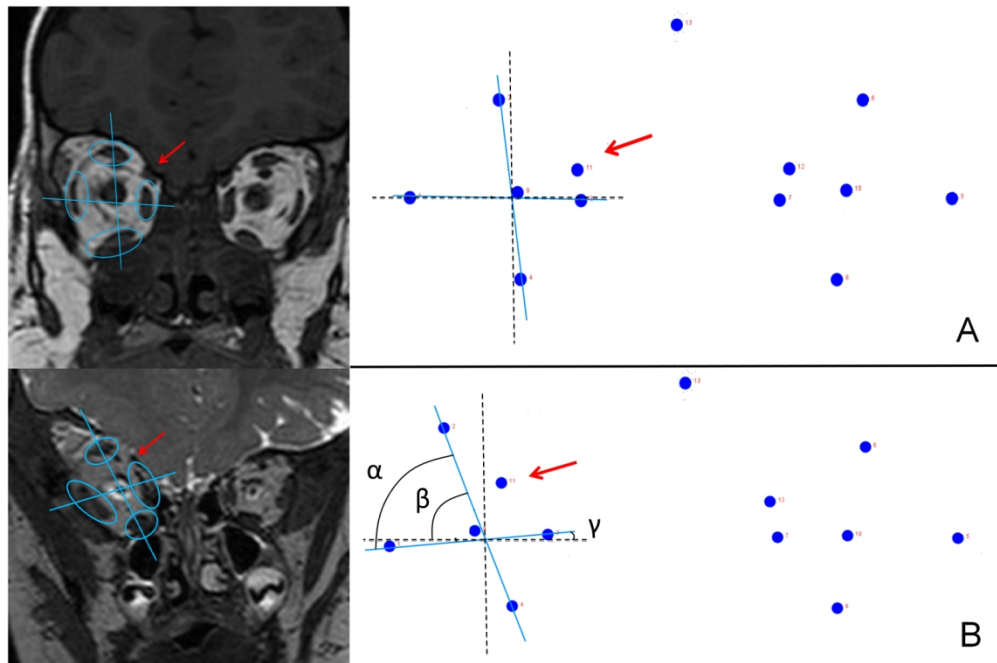


Figure 2. A. Procrustes superimposition in axial view for controls; right trochlea of the superior oblique muscle: red arrow. B. Procrustes superimposition in coronal view for controls; right trochlea of the superior oblique muscle: red arrow. C. Procrustes superimposition in sagittal view for controls. D. Procrustes superimposition in axial view for anterior plagiocephaly; right trochlea of the superior oblique muscle: red arrow. E. Procrustes superimposition in coronal view for anterior plagiocephaly; right trochlea of the superior oblique muscle: red arrow. F. Procrustes superimposition in sagittal view for anterior plagiocephaly.



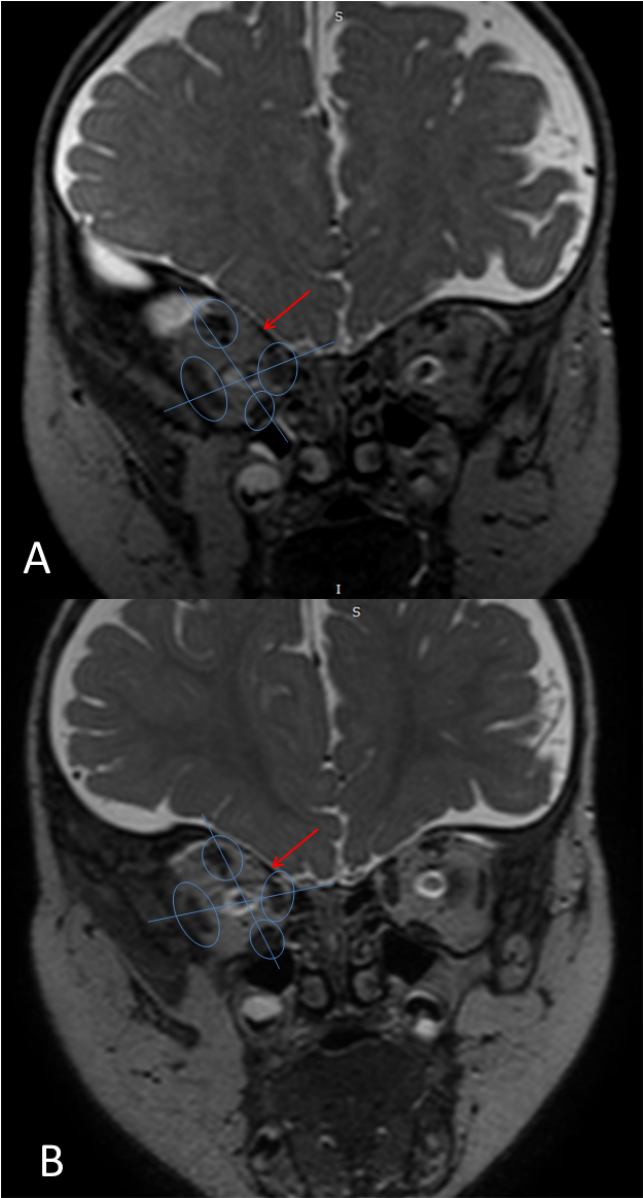
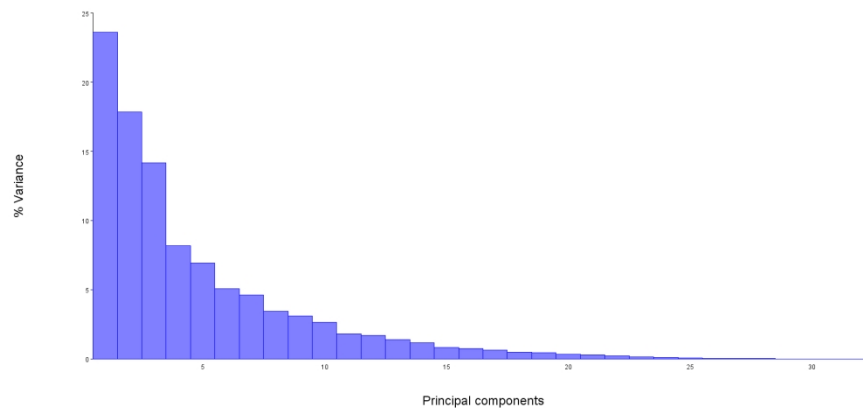


Figure 4. A. Coronal MRI section in anterior plagiocephaly before fronto-orbital advancement. B. Coronal MRI section in anterior plagiocephaly after fronto-orbital advancement. Qualitative correction of the position of the right trochlea of the superior oblique muscle (red arrow) and qualitative reduction of the excyclorotation of recti muscles.



672x310mm (72 x 72 DPI)

